Robustness of chimera states in nonlocally coupled networks of nonidentical logistic maps

Anne-Kathleen Malchow,[1] Iryna Omelchenko,[1] Eckehard Schöll,[1] and Philipp Hövel[1,2,*]
[1]*Institut für Theoretische Physik, Technische Universität Berlin, Hardenbergstraße 36, 10623 Berlin, Germany*
[2]*Bernstein Center for Computational Neuroscience Berlin, Humboldt-Universität zu Berlin, Philippstraße 13, 10115 Berlin, Germany*

(Received 25 May 2018; published 30 July 2018)

We investigate the dynamics of nonlocally coupled time-discrete maps with emphasis on the occurrence and robustness of chimera states. These peculiar, hybrid states are characterized by a coexistence of coherent and incoherent regions. We consider logistic maps coupled on a one-dimensional ring with finite coupling radius. Domains of chimera existence form different tongues in the parameter space of coupling range and coupling strength. For a sufficiently large coupling strength, each tongue refers to a wave number describing the structure of the spatial profile. We also analyze the period-adding scheme within these tongues and multiplicity of period solutions. Furthermore, we study the robustness of chimeras with respect to parameter inhomogeneities and find that these states persist for different widths of the parameter distribution. Finally, we explore the spatial structure of the chimera using a spatial correlation function.

DOI: 10.1103/PhysRevE.98.012217

I. INTRODUCTION

Systems of coupled oscillators can exhibit a wide range of complex dynamics, even if the dynamics of the individual oscillator are fairly simple, and a long list of research efforts in nonlinear sciences focus on patterns of synchrony [1–7]. Especially the two cases of global (all-to-all) and local (nearest neighbor) coupling have been thoroughly investigated [8–13], as well as an intermediate case of nonlocal coupling, where every node of the network is coupled to a fixed number of neighbors [14–16]. A particularly interesting, self-organized phenomenon that occurs in these networks is the emergence of chimera states. These peculiar states show a hybrid spatial structure, which is partially coherent and partially incoherent. They have first been observed in networks of coupled phase oscillators [17,18] and their universal appearance has been established for a wide range of different time-continuous models [19–33]; for recent reviews see [25,34]. At first chimera states were studied only by numerical simulations. Later, chimera states were also realized in different experiments, including lattices of coupled optical [35], chemical [36], and mechanical [37] oscillators, optoelectronic feedback loops [38–40], and electrochemical [41,42] and electronic oscillators [43]. The robustness of chimera states against perturbations to the network structure through random removal of links was studied in Ref. [44]. Perturbations of the coupling kernel [45] or local parameters of a few elements [46] can be used to control the position of the coherent and incoherent regions. Feedback control based on the measurement of the order parameter allows for the extension of chimera lifetime and stabilization of its spatial position even for small networks [19,47,48]. Inhomogeneity of network elements, that is, variations of the system parameters, has also been considered, e.g., for coupled FitzHugh-Nagumo and Van der Pol oscillators [48,49].

In addition to and in contrast to the above mentioned time-continuous models, time-discrete systems have also been considered [35,50–59]. Therein, the network elements are described by chaotic or periodic maps, and chimera-like states can be observed as well. Again, they exhibit the typical hybrid spatial structure of partial coherence and partial incoherence, with the incoherent parts displaying spatial chaos, while their temporal behavior is periodic, even if the isolated maps operate in the chaotic regime.

Considering both time-discrete maps and time-continuous flows, Semonova *et al.* have shown that chimera states can be found in networks of oscillators that fall in the class of nonhyperbolic chaotic attractors, but not in networks of systems with hyperbolic chaotic attractors [56]. The former includes the logistic map, which will be considered below, the Henon map [52], and the time-continuous Rössler system [54,58]. Examples for latter class are the Lozi map and the Lorenz system [56].

In this paper, we investigate the influence of inhomogeneous parameters in time-discrete maps on the existence of chimera states. For this purpose, we study the case of a nonlocally coupled network of nonidentical logistic maps. For identical systems, we also elucidate details concerning the multiplicity of solutions of the same period. In addition, we study the profile by means of a spatial correlation function.

The rest of the paper is organized as follows: In Sec. II, we introduce the model equations. In Sec. III, after a brief review of results and new aspects on coupled identical systems, we present our findings for nonidentical systems, where we consider different amounts of parameter inhomogeneity. In particular, we discuss the transition from spatial coherence to incoherence on the basis of stability diagrams, snapshots, space-time plots, the local order parameter, and bifurcation diagrams. We will show that even for a highly nonidentical system, chimera-shaped states can still exist. We add some considerations on the analysis of the spatial structure of chimeras and, finally, summarize our study in Sec. IV.

*phoevel@physik.tu-berlin.de

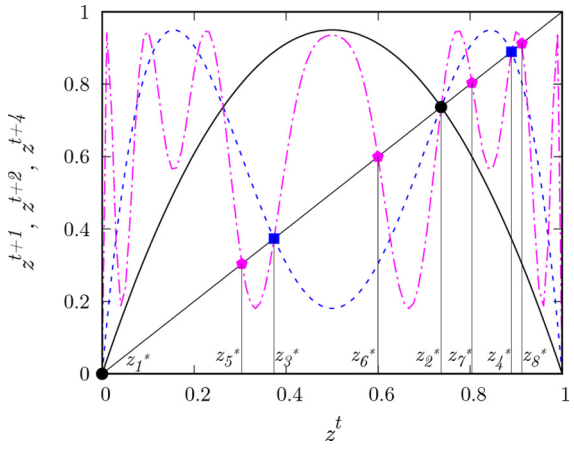

FIG. 1. Original (solid), twice iterated [$f^{(2)}(z)$, dashed blue], and quadruple iterated [$f^{(4)}(z)$, dash-dotted magenta] map and its fixed points z_1^* to z_8^*. Parameter: $a = 3.8$.

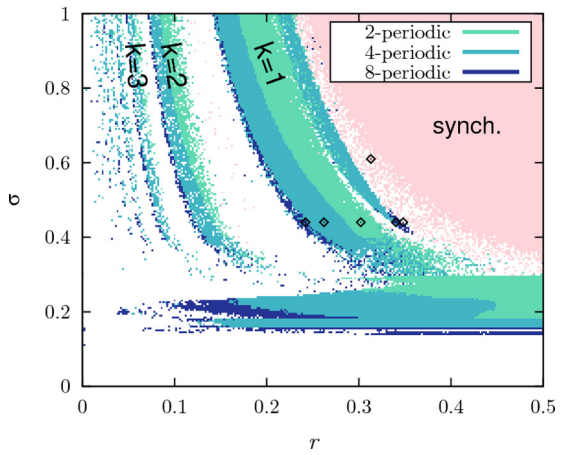

FIG. 2. Regions of temporal periodicity in the (r, σ)-parameter plane. Green (light gray), light blue (dark gray), and blue (black) colors mark regions of periods 2, 4, and 8, respectively. In the light red (pale gray, marked as *synch.*) region, chaotic synchronization occurs. The stability tongues are labeled with the respective wave number k of their wave-like profiles. Parameters: $N = 500$, $a = 3.8$.

II. MODEL

The system to be considered in the following consists of N real-valued, single-variable time-discrete maps that are coupled to each other in a network of translational invariance:

$$z_i^{t+1} = f(z_i^t, a_i) + \frac{\sigma}{2P} \sum_{j=i-P}^{i+P} \left[f(z_j^t, a_j) - f(z_i^t, a_i) \right]. \quad (1)$$

The local dynamics of every element i on a one-dimensional ring is described by a logistic map $f(z_i, a_i) = a_i z_i (1 - z_i)$, assigned with potentially different, but fixed nonlinearity parameter a_i. All other properties of the network remain unchanged. The inhomogeneities in the parameters are realized according to a Gaussian distribution with a mean value of $\langle a \rangle = 3.8$ and varying standard deviations s. Values outside the interval [0,4] are neglected to ensure a mapping to the interval $z_i^{t+1} \in [0, 1]$.

Fixed points of the time-discrete map satisfy $z^{t+1} = f(z^t, a) = z^t$ and, similarly, solutions of period n are given by $z^{t+n} = f^{(n)}(z^t) = z^t$, where $f^{(n)}(z)$ denotes the nth iterate of f. See Fig. 1 for an illustration of the original (solid line), twice iterated map $f(f(z^t))$ (dashed line), and quadruple iterated map $f^{(4)}(z)$ (dash-dotted line).

The considered coupling scheme has periodic boundary conditions realized as a one-dimensional ring, that is, all indexes have to be taken modulo N. Every oscillator is coupled to a fixed number P of nearest neighbors to either side along the ring. For $P = 1$, when the elements are only coupled to their two next neighbors, one obtains local, nearest-neighbor coupling. All-to-all or global coupling is achieved by $P = \frac{N}{2}$ ($P = \frac{N-1}{2}$ assuming odd N). Every case in between is regarded as nonlocal coupling. This leads to the definition of the coupling radius r by $r = \frac{P}{N}$, which ranges from $r = \frac{1}{N}$ to $r = 0.5$ for local or global coupling, respectively. The extent of influence of the neighboring elements can be adjusted by the coupling strength σ, within the interval (0,1).

Generally, the nonlinearity parameter a can be different for every element. However, in order to demonstrate the robustness, we will first review the identical case with fixed a, considered in [58,59], and then discuss the influence of inhomogeneity in this parameter. Note that the value of the nonlinearity parameter a defines the type of dynamics for each individual node. For the case of identical maps, we consider a value of a in the chaotic regime. Adding inhomogeneity yields the case of nonidentical maps, in which some of the values of parameters a_i can correspond to the periodic windows of the logistic map. Even if all maps in the nonlocally coupled network operate in the periodic regime, chimera states can be observed [59]. The time periodicity of the solutions can, however, differ from the chaotic case. In the present study, we demonstrate that chimera states can be robust, even when the network consists of a mixture of chaotic and periodic local dynamics.

III. RESULTS

Figure 2 displays a stability diagram in the (r, σ)-parameter plane for $a = 3.8$ (cf. Ref. [59]). In every point of the diagram, the same random initial conditions have been used, and the first 1000 time steps have been neglected as transient time.

Let us briefly review the main features of the stability diagram [59]. In the region of a highly coupled network the states of chaotic synchronization can be found, indicated by light red color (pale gray, marked as *synch.*). For strong and long-ranged coupling, the network dynamics is synchronous in space, but chaotic in time. The colored stability tongues stand for time periodic states, where green (light gray), light blue (dark gray), and blue (black) colors denote 2-, 4-, and 8-periodicity, respectively. Hence, with decreasing coupling strength and radius, the system undergoes a cascade of bifurcations at the region boundaries, each one causing a period-doubling in time. As the coupling strength σ decreases, the system undergoes a transition from coherence to incoherence at σ_{crit}. In Ref. [58] an approximation for $\sigma_{\text{crit}} \approx 1 - \frac{1}{a-2}$ has been derived analytically for the case of time-periodic states. For $a = 3.8$, this yields $\sigma_{\text{crit}} \approx 0.44$. Below this critical value, the state loses coherence and the former wave-like profile breaks

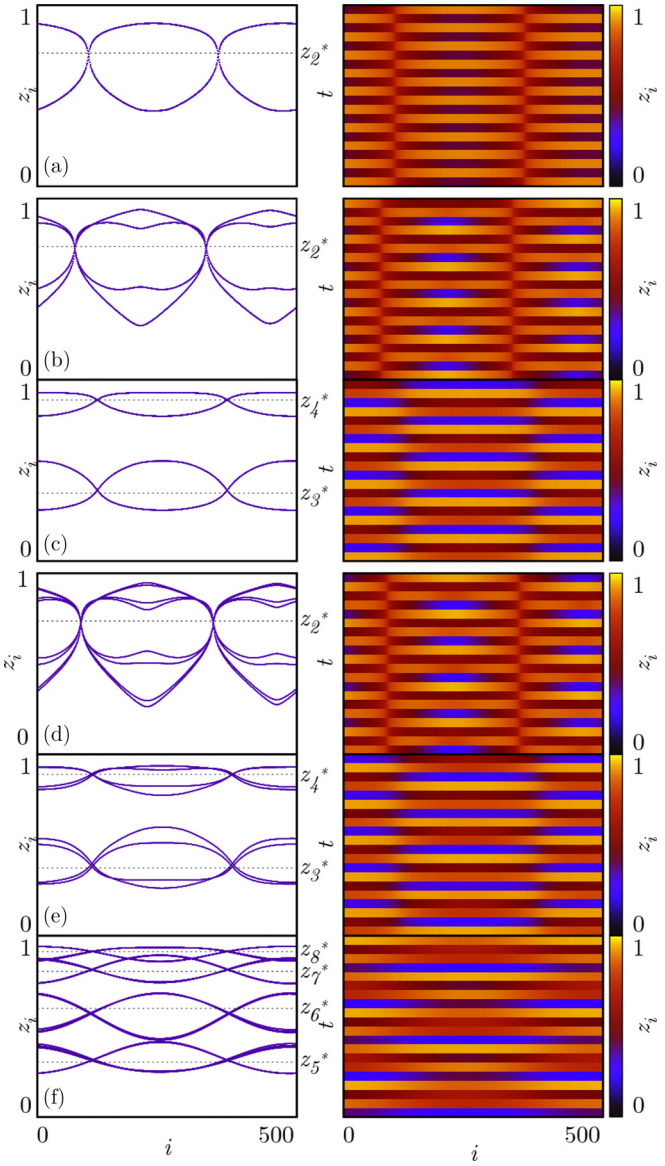

FIG. 3. Stacked snapshots and space-time plots for different coupling ranges (a) $r = 0.242$, (b) 0.262, (c) 0.302, (d) 0.340, (e) 0.348 with fixed coupling strength $\sigma = 0.44$, and (f) $r = 0.313$ with $\sigma = 0.61$, corresponding to the diamonds in Fig. 2. The dotted lines mark the value of the fixed point of the original and iterated maps. Other parameters as in Fig. 2.

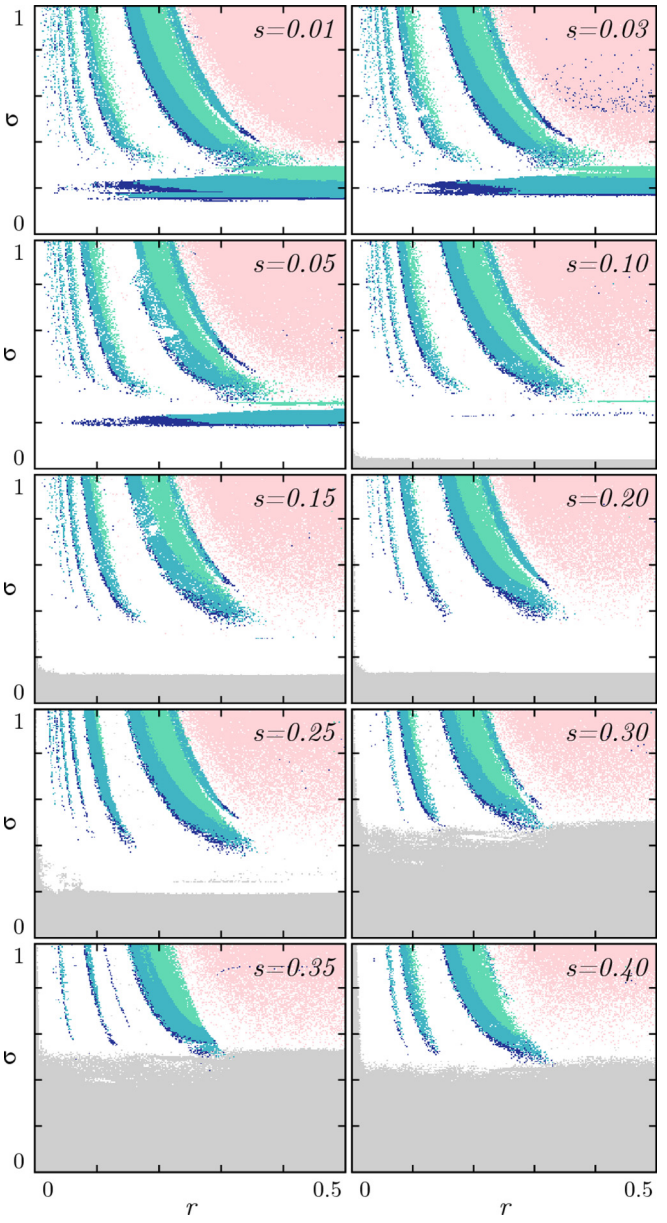

FIG. 4. Stability diagrams in the (r, σ)-parameter plane for the Gaussian distributed a_i with mean value $\langle a \rangle = 3.8$ and 10 different values of the standard deviation s. Other parameters and color code as in Fig. 2.

up into two parts: one upper and one lower branch. With further decrease of σ, the incoherent parts around the breaking points grow larger, while the inner parts of the branches stay coherent. Eventually, the incoherence has spread over the entire network.

Figure 3 shows stacked snapshots and space-time plots for different examples of the $k = 1$ wave solution. Parameters are chosen as fixed coupling strength $\sigma = 0.44$ and different coupling ranges, except for panel (f), which corresponds to $\sigma = 0.61$. The snapshots consist of overlays of 20 time steps to visualize the temporal periodicity. It can be seen that solutions of period 4, 8, ... emerge from different profiles. The period-4 states, for instance, are generated by period doubling from the period-2 state. See Figs. 3(a) to 3(c).

Since the profiles are stationary and do not drift along the ring, some nodes act as joints, whose values z^t do not change over time. Interestingly, the value of the these joint nodes is given by the fixed point z_2^* of the original map as in panels (a), (b), and (d) (cf. Fig. 1). Alternatively, they can exhibit period-2 behavior and agree with the fixed points of the twice iterated map (z_3^* and z_4^*) as in panels (c) and (e). Similarly, the period-8 states might arise from period-2 and period-4 solutions, where the joint nodes take values which are in good agreement with the fixed points of the original and twice iterated map as shown in Figs. 3(d) and 3(e), respectively. We also observe solutions where the z^t value of the joint nodes in the period-8 state are close to the fixed points of the quadruple iterated map (z_5^*, z_6^*, z_7^*, and z_8^* in Fig. 1). See Fig. 3(f).

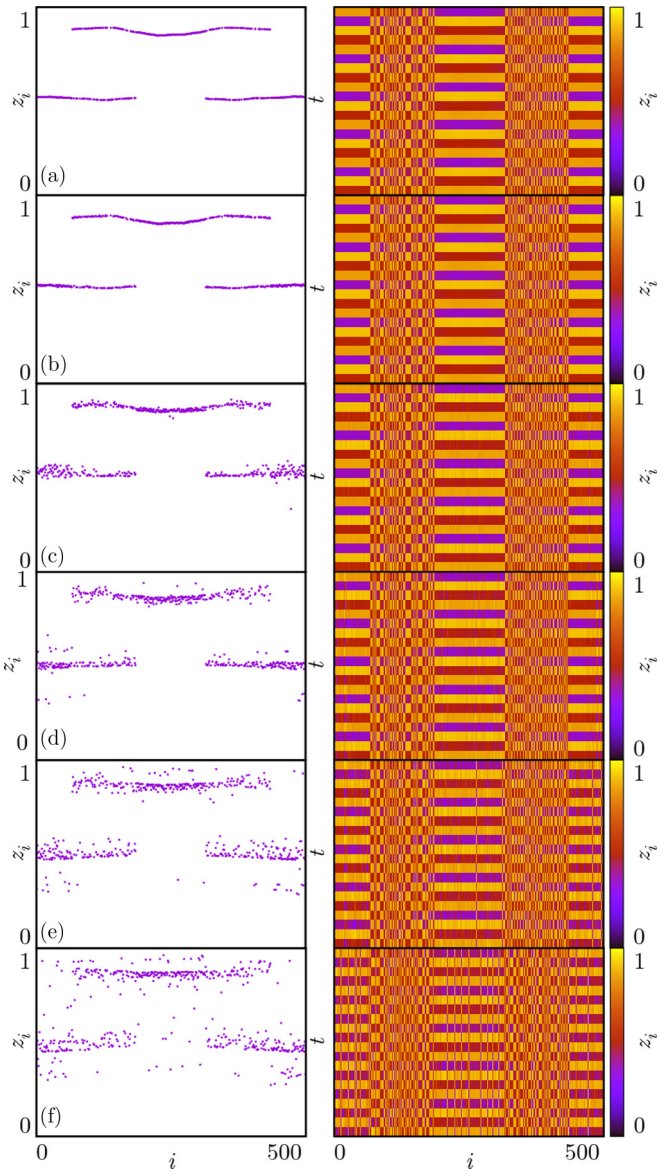

FIG. 5. Snapshots and space-time profiles for a mean value $\langle a \rangle = 3.8$ and different standard deviations $s = 0$, 0.01, 0.05, 0.1, 0.15, and 0.2 in panels (a) to (f), respectively. Other parameters: $r = 0.32$, $\sigma = 0.22$.

To describe the properties of a chimera state more quantitatively, the local order parameter is used. It can be calculated for a state snapshot and is defined as

$$R_j = \lim_{N\to\infty} \frac{1}{2\delta} \left| \sum_{\left|\frac{k}{N} - \frac{j}{N}\right| \leqslant \delta} e^{i\Psi_k} \right| \qquad (j = 1, \ldots, N) \qquad (2)$$

[59,60]. It is a measure of the local coherence of the network because, for an element i, it considers every neighboring element j within a certain range, determined by δ. The phase Ψ_j is given by

$$\sin \Psi_j = \frac{2z_j - \max_j z_j - \min_j z_j}{\max_j z_j - \min_j z_j}. \qquad (3)$$

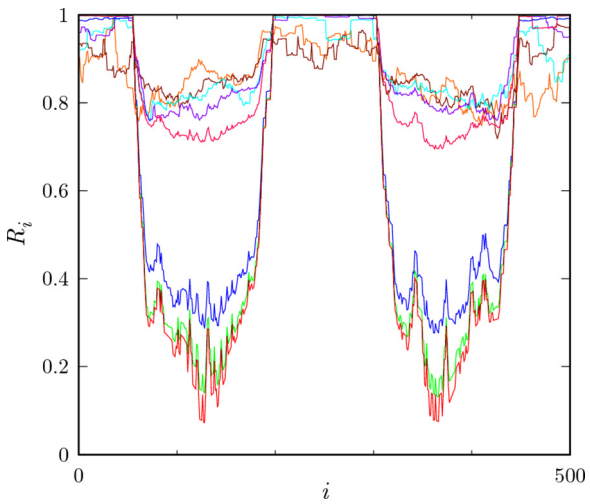

FIG. 6. Local order parameter of different standard deviations s: $s = 0$ (red), 0.01 (green), 0.03 (blue), 0.05 (light red), 0.1 (purple), 0.15 (cyan), 0.2 (brown), and 0.25 (orange). Other parameters and corresponding dynamics are as in Fig. 5.

This yields that R_i lies in the interval [0,1], where high values close to unity denote spatial coherence. In incoherent parts, R_i decreases significantly. Equation (2) can only be approximated by the considered system, as it contains a finite number of $N = 500$ elements. With a choice of $\delta = 0.025$, as in Ref. [59], the local order parameter is computed as an average of 12 neighbors.

Let us now consider the case of inhomogeneous nonlinearity parameters. In Fig. 4, the stability diagrams for various widths s of the Gaussian distribution are plotted. Realizations that cause divergences ($z_i^{t+1} \notin [0, 1]$) due to parameter values outside the interval $a_i \in [0, 4]$ are neglected (light gray region for small coupling strengths). The introduction of inhomogeneities generally has most influence on the regions of small coupling strength σ. First, the incoherent time-periodic region in the lower parts shrinks until it vanishes for $s \approx 0.10$. With growing inhomogeneity, the tongues for large k vanish as well. The $k = 1$ and $k = 2$ tongues are increasingly reduced in length in the direction of σ.

To illustrate the influence of parameter fluctuations, we fix the coupling range and strength at $r = 0.32$ and $\sigma = 0.22$ and vary the standard deviation in Fig. 5. The first column depicts the snapshots and the second column shows the corresponding space-time plots. It can be observed that the general shape of the profile is kept in spite of the inhomogeneity, although it becomes blurred.

This effect can be further quantified using the local order parameter defined in Eq. (2). Figure 6 depicts the profiles of R_i for the chimera state at $\sigma = 0.22$ in the identical case ($s = 0$, red curve) and several nonidentical cases. The respective snapshots are depicted in Fig. 5. It can be seen that the states maintain the typical shape of the local order parameter for small values of the standard deviation s (cf. Ref. [59]). Then, between $s = 0.03$ and 0.05, a qualitative change happens and the curves flatten, becoming much less distinct due to increased parameter fluctuations.

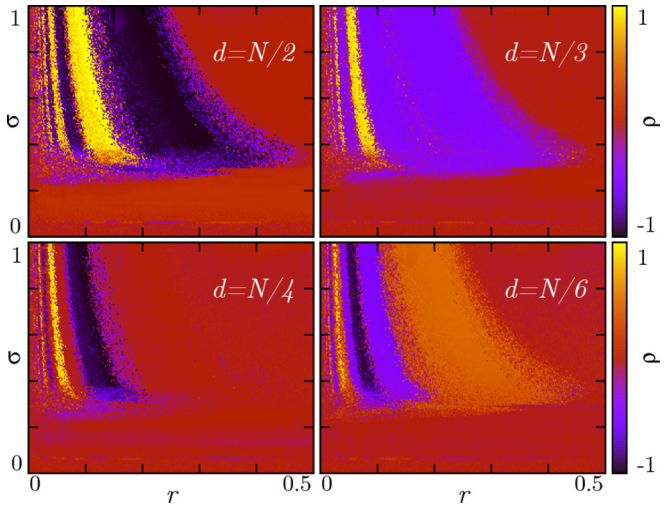

FIG. 7. Correlation coefficients ρ of a snapshot and its shifted version in the (r, σ)-parameter plane for different values of the shift d. Parameters a_i are normally distributed with a standard deviation $s = 0.01$.

To illustrate that the regions of the stability diagram indeed coincide with regions of spatial periodicity, we present spatial correlation diagrams next. They are obtained by comparing the profile of a state with its shifted replica resulting in a correlation coefficient,

$$\rho_{X,Y} = \frac{\mathrm{cov}(X, Y)}{\sigma_X \sigma_Y} = \frac{\langle XY\rangle - \langle X\rangle\langle Y\rangle}{\sqrt{\langle X^2\rangle - \langle X\rangle^2}\sqrt{\langle Y^2\rangle - \langle Y\rangle^2}}. \quad (4)$$

Here, X and Y stand for the two data sets of the profiles to be compared, $\langle X\rangle$ and $\langle Y\rangle$ are their mean values, and σ_X and σ_Y their standard deviations. Note that a cross-correlation analysis has been proposed in Ref. [55] to study the spatial coherence of chimera states. Here, we aim to investigate the spatial periodicity of a state. For this purpose, X is chosen as the profile and Y is the same profile shifted by d. Since a system with periodic boundary conditions is considered, the shifting can be realized by $Y : z^Y_{(i+d) \bmod N} = z^X_i \ \forall i$. The shift d is varied in the range $d = N/2, N/3, \ldots, N/8$ to account for periods of 2 to 8. The value of $\rho_{X,Y}$ lies within the interval $[-1, 1]$, where $\rho_{X,Y} = 1$ indicates complete periodicity, $\rho_{X,Y} = -1$ means antiphase periodicity, and for $\rho_{X,Y} = 0$ no resemblance in terms of linear correlation is found at all.

The correlation coefficient $\rho_{X,Y}$ is a comparatively sensitive method for the detecting of the stability tongues referring to different wave numbers in the (r, σ)-parameter plane, as shown in Fig. 7. Shifts of $d = N/m$ with $m = 1, 2, 3, \ldots$ show a high correlation for profiles with wave numbers $k = m$ or integer multiples thereof and high anticorrelation for profiles with $k = m/2, 3m/2, \ldots$ if m is even.

IV. CONCLUSION

In the current study we have demonstrated how nonidentical nodes influence chimera states in networks of nonlocally coupled logistic maps. The observed chimera-like states are spatially hybrid states, which are partially coherent and partially incoherent and exhibit time-periodic behavior. The single logistic maps have been modified by potentially different but fixed nonlinearity parameters to create an inhomogeneous system. For this purpose, Gaussian distributed parameters, with a mean value which lies in the chaotic regime and different standard deviations, have been used. The considered regular network configuration is a nonlocally coupled ring described by the coupling radius r, which defines with how many neighbors each element is coupled in either direction of a one-dimensional ring, and the coupling strength σ.

We have computed stability diagrams in the (r, σ)-parameter plane and compared for different degrees of inhomogeneities. To investigate the emergence of chimera states for nonidentical systems, we have explored the coherence-incoherence transition and observed chimera-shaped states for various extents of inhomogeneity. We have found that the positions of the stability regions and the regions of chimera states mainly depend on the mean value of the nonlinearity parameter, in agreement with analytical results reported in Ref. [58]. The regions of spatial and temporal periodicity coincide even for highly inhomogeneous cases. Furthermore, an additional region of states with temporal periods 4 and 8 was discovered for the spatial wave-like profile of wave number $k = 1$. In previous works, this region was reported for the time-continuous Rössler model, but not for time-discrete maps [59].

We have further characterized the observed dynamics using the local order parameter as a measure of coherence. For standard deviations of the Gaussian distributed system parameters up to $s = 0.03$, the chimera states mainly retain their characteristic properties. For greater s, they gradually fade. Furthermore, we have illustrated the effects of parameter inhomogeneities by snapshots and space-time profiles.

Our findings provide insight into the robustness of chimera states and demonstrate that chimera patterns persist for inhomogeneous parameters.

ACKNOWLEDGMENT

This work was supported by Deutsche Forschungsgemeinschaft in the framework of Collaborative Research Center SFB 910.

[1] F. A. Rodrigues, T. K. D. Peron, P. Ji, and J. Kurths, The Kuramoto model in complex networks, Phys. Rep. **610**, 1 (2016).

[2] D. M. Abrams, L. M. Pecora, and A. E. Motter, Introduction to focus issue: Patterns of network synchronization, Chaos **26**, 094601 (2016).

[3] K. Kaneko, From globally coupled maps to complex-systems biology, Chaos **25**, 097608 (2015).

[4] A. Arenas, A. Díaz-Guilera, J. Kurths, Y. Moreno, and C. Zhou, Synchronization in complex networks, Phys. Rep. **469**, 93 (2008).

[5] *Handbook of Chaos Control*, 2nd ed., edited by E. Schöll and H. G. Schuster (Wiley-VCH, Weinheim, 2008).

[6] A. Pikovsky, M. Rosenblum, and J. Kurths, *Synchronization: A Universal Concept in Nonlinear Sciences*, Vol. 12 (Cambridge Univerity Press, Cambridge, 2003).

[7] S. Boccaletti, J. Kurths, G. Osipov, D. L. Valladares, and C. S. Zhou, The synchronization of chaotic systems, Phys. Rep. **366**, 1 (2002).

[8] A. Yeldesbay, A. Pikovsky, and M. Rosenblum, Chimeralike States in an Ensemble of Globally Coupled Oscillators, Phys. Rev. Lett. **112**, 144103 (2014).

[9] J. Ladenbauer, J. Lehnert, H. Rankoohi, T. Dahms, E. Schöll, and K. Obermayer, Adaptation controls synchrony and cluster states of coupled threshold-model neurons, Phys. Rev. E **88**, 042713 (2013).

[10] P. Ashwin, O. Burylko, Y. Maistrenko, and O. Popovych, Extreme Sensitivity to Detuning for Globally Coupled Phase Pscillators, Phys. Rev. Lett. **96**, 054102 (2006).

[11] V. Afraimovich, *Some Topological Properties of Lattice Dynamical Systems*, Lecture Notes in Physics Vol. 671 (Springer, Berlin, 2005), p. 153.

[12] I. Matskiv, Y. Maistrenko, and E. Mosekilde, Synchronization between interacting ensembles of globally coupled chaotic maps, Physica D **199**, 45 (2004).

[13] A. Pikovsky, O. Popovych, and Y. Maistrenko, Resolving Clusters in Chaotic Ensembles of Globally Coupled Identical Oscillators, Phys. Rev. Lett. **87**, 044102 (2001).

[14] J. Siebert, S. Alonso, M. Bär, and E. Schöll, Dynamics of reaction-diffusion patterns controlled by asymmetric nonlocal coupling as limiting case of differential advection, Phys. Rev. E **89**, 052909 (2014).

[15] V. Dziubak, Y. Maistrenko, and E. Schöll, Coherent traveling waves in nonlocally coupled chaotic systems, Phys. Rev. E **87**, 032907 (2013).

[16] G. C. Sethia and A. Sen, Existence and stability of traveling-wave states in a ring of nonlocally coupled phase oscillators with propagation delays, Phys. Rev. E **84**, 066203 (2011).

[17] Y. Kuramoto and D. Battogtokh, Coexistence of coherence and incoherence in nonlocally coupled phase oscillators, Nonliear Phenom. Complex Syst. **5**, 380 (2002).

[18] D. M. Abrams and S. H. Strogatz, Chimera States for Coupled Oscillators, Phys. Rev. Lett. **93**, 174102 (2004).

[19] I. Omelchenko, O. E. Omel'chenko, A. Zakharova, and E. Schöll, Optimal design of tweezer control for chimera states, Phys. Rev. E **97**, 012216 (2018).

[20] S. Ghosh, A. Zakharova, and S. Jalan, Non-identical multiplexing promotes chimera states, Chaos Solitons Fractals **106**, 56 (2018).

[21] J. Shena, J. Hizanidis, P. Hövel, and G. P. Tsironis, Multi-clustered chimeras in large semiconductor laser arrays with nonlocal interactions, Phys. Rev. E **96**, 032215 (2017).

[22] N. D. Tsigkri-DeSmedt, J. Hizanidis, E. Schöll, P. Hövel, and A. Provata, Chimeras in leaky integrate-and-fire neural networks: effects of reflecting connectivities, Eur. Phys. J. B **90**, 139 (2017).

[23] J. Hizanidis, N. E. Kouvaris, G. Zamora-López, A. Díaz-Guilera, and C. Antonopoulos, Chimera-like states in modular neural networks, Sci. Rep. **6**, 19845 (2016).

[24] E. A. Martens, M. J. Panaggio, and D. M. Abrams, Basins of attraction for chimera states, New J. Phys. **18**, 022002 (2016).

[25] M. J. Panaggio and D. M. Abrams, Chimera states: Coexistence of coherence and incoherence in networks of coupled oscillators, Nonlinearity **28**, R67 (2015).

[26] A. Vüllings, J. Hizanidis, I. Omelchenko, and P. Hövel, Clustered chimera states in systems of type-I excitability, New J. Phys. **16**, 123039 (2014).

[27] J. Hizanidis, V. Kanas, A. Bezerianos, and T. Bountis, Chimera states in networks of nonlocally coupled Hindmarsh-Rose neuron models, Int. J. Bifurcation Chaos **24**, 1450030 (2014).

[28] O. E. Omel'chenko, Coherence-incoherence patterns in a ring of non-locally coupled phase oscillators, Nonlinearity **26**, 2469 (2013).

[29] M. Wolfrum, O. E. Omel'chenko, S. Yanchuk, and Y. Maistrenko, Spectral properties of chimera states, Chaos **21**, 013112 (2011).

[30] O. E. Omel'chenko, M. Wolfrum, and Y. Maistrenko, Chimera states as chaotic spatiotemporal patterns, Phys. Rev. E **81**, 065201(R) (2010).

[31] C. R. Laing, Chimera states in heterogeneous networks, Chaos **19**, 013113 (2009).

[32] G. C. Sethia, A. Sen, and F. M. Atay, Clustered Chimera States in Delay-Coupled Oscillator Systems, Phys. Rev. Lett. **100**, 144102 (2008).

[33] T. W. Ko and G. B. Ermentrout, Partially locked states in coupled oscillators due to inhomogeneous coupling, Phys. Rev. E **78**, 016203 (2008).

[34] E. Schöll, Synchronization patterns and chimera states in complex networks: Interplay of topology and dynamics, Eur. Phys. J. Spec. Top. **225**, 891 (2016) (special issue on Mathematical Modeling of Complex Systems, edited by T. Bountis, A. Provata, G. Tsironis, and J. Johnson).

[35] A. M. Hagerstrom, T. E. Murphy, R. Roy, P. Hövel, I. Omelchenko, and E. Schöll, Experimental observation of chimeras in coupled-map lattices, Nat. Phys. **8**, 658 (2012).

[36] M. R. Tinsley, S. Nkomo, and K. Showalter, Chimera and phase cluster states in populations of coupled chemical oscillators, Nat. Phys. **8**, 662 (2012).

[37] E. A. Martens, S. Thutupalli, A. Fourriere, and O. Hallatschek, Chimera states in mechanical oscillator networks, Proc. Natl. Acad. Sci. USA **110**, 10563 (2013).

[38] L. Larger, B. Penkovsky, and Y. Maistrenko, Virtual Chimera States for Delayed-Feedback Systems, Phys. Rev. Lett. **111**, 054103 (2013).

[39] L. Larger, B. Penkovsky, and Y. Maistrenko, Laser chimeras as a paradigm for multistable patterns in complex systems, Nat. Commun. **6**, 7752 (2015).

[40] J. D. Hart, D. C. Schmadel, T. E. Murphy, and R. Roy, Experiments with arbitrary networks in time-multiplexed delay systems, Chaos **27**, 121103 (2017).

[41] M. Wickramasinghe and I. Z. Kiss, Spatially organized dynamical states in chemical oscillator networks: Synchronization, dynamical differentiation, and chimera patterns, PLoS ONE **8**, e80586 (2013).

[42] L. Schmidt, K. Schönleber, K. Krischer, and V. Garcia-Morales, Coexistence of synchrony and incoherence in oscillatory media under nonlinear global coupling, Chaos **24**, 013102 (2014).

[43] L. V. Gambuzza, A. Buscarino, S. Chessari, L. Fortuna, R. Meucci, and M. Frasca, Experimental investigation of chimera states with quiescent and synchronous domains in coupled electronic oscillators, Phys. Rev. E **90**, 032905 (2014).

[44] N. Yao, Z.-G. Huang, Y.-C. Lai, and Z. Zheng, Robustness of chimera states in complex dynamical systems, Sci. Rep. **3**, 3522 (2013).

[45] C. Bick and E. A. Martens, Controlling chimeras, New J. Phys. **17**, 033030 (2015).

[46] T. M. Isele, J. Hizanidis, A. Provata, and P. Hövel, Controlling chimera states: The influence of excitable units, Phys. Rev. E **93**, 022217 (2016).

[47] J. Sieber, O. E. Omel'chenko, and M. Wolfrum, Controlling Unstable Chaos: Stabilizing Chimera States by Feedback, Phys. Rev. Lett. **112**, 054102 (2014).

[48] I. Omelchenko, O. E. Omel'chenko, A. Zakharova, M. Wolfrum, and E. Schöll, Tweezers for Chimeras in Small Networks, Phys. Rev. Lett. **116**, 114101 (2016).

[49] I. Omelchenko, A. Provata, J. Hizanidis, E. Schöll, and P. Hövel, Robustness of chimera states for coupled FitzHugh-Nagumo oscillators, Phys. Rev. E **91**, 022917 (2015).

[50] A. zur Bonsen, I. Omelchenko, A. Zakharova, and E. Schöll, Chimera states in networks of logistic maps with hierarchical connectivities, Eur. Phys. J. B **91**, 65 (2018).

[51] I. A. Shepelev, A. V. Bukh, G. I. Strelkova, T. E. Vadivasova, and V. S. Anishchenko, Chimera states in ensembles of bistable elements with regular and chaotic dynamics, Nonlinear Dyn. **90**, 2317 (2017).

[52] N. Semenova, G. Strelkova, V. S. Anishchenko, and A. Zakharova, Temporal intermittency and the lifetime of chimera states in ensembles of nonlocally coupled chaotic oscillators, Chaos **27**, 061102 (2017).

[53] A. Bukh, E. Rybalova, N. Semenova, G. Strelkova, and V. Anishchenko, New type of chimera and mutual synchronization of spatiotemporal structures in two coupled ensembles of nonlocally interacting chaotic maps, Chaos **27**, 111102 (2017).

[54] S. Bogomolov, A. Slepnev, G. Strelkova, E. Schöll, and V. S. Anishchenko, Mechanisms of appearance of amplitude and phase chimera states in a ring of nonlocally coupled chaotic systems, Commun. Nonlinear Sci. Numer. Simul. **43**, 25 (2017).

[55] T. E. Vadivasova, G. Strelkova, S. A. Bogomolov, and V. S. Anishchenko, Correlation analysis of the coherence-incoherence transition in a ring of nonlocally coupled logistic maps, Chaos **26**, 093108 (2016).

[56] N. Semenova, A. Zakharova, E. Schöll, and V. S. Anishchenko, Does hyperbolicity impede emergence of chimera states in networks of nonlocally coupled chaotic oscillators? Europhys. Lett. **112**, 40002 (2015).

[57] D. Dudkowski, Y. Maistrenko, and T. Kapitaniak, Different types of chimera states: An interplay between spatial and dynamical chaos, Phys. Rev. E **90**, 032920 (2014).

[58] I. Omelchenko, B. Riemenschneider, P. Hövel, Y. Maistrenko, and E. Schöll, Transition from spatial coherence to incoherence in coupled chaotic systems, Phys. Rev. E **85**, 026212 (2012).

[59] I. Omelchenko, Y. Maistrenko, P. Hövel, and E. Schöll, Loss of Coherence in Dynamical Networks: Spatial Chaos and Chimera states, Phys. Rev. Lett. **106**, 234102 (2011).

[60] M. Wolfrum and O. E. Omel'chenko, Chimera states are chaotic transients, Phys. Rev. E **84**, 015201 (2011).